RSC Advances

Dynamic Article Links ►

Cite this: DOI: 10.1039/c0xx00000x

www.rsc.org/xxxxxx

ARTICLE TYPE

The distinct role of the flexible polymer matrix in catalytic conversions over immobilised nanoparticles

Stefano Martinuzzi,[a] Daniela Cozzula,[b] Paulo Centomo,[a] Marco Zecca,*[a] and Thomas E. Müller*[b]

Received (in XXX, XXX) Xth XXXXXXXXX 20XX, Accepted Xth XXXXXXXXX 20XX

DOI: 10.1039/b000000x

Supplementary Material

Materials

The K1221 resin was obtained from Lanxess; active carbon was obtained from Evonik. Aniline (99.5%), cyclohexylamine (99%), methanol (anhydrous, 99.8%), $NaBH_4$ (98%), nitrobenzene (>99%), 2-propanol (99.5%), NaOH, THF (>99%), all metal precursors ($Ni(OAc)_2$ $4H_2O$, 98%; $[Pt(NH_3)_4](NO_3)_2$, 99.995%; $Rh(NO_3)_3$ in 5%$_{w/w}$ HNO_3, Rh 10%$_{w/w}$; aqueous $Ru(NO)(NO_3)_x(OH)_y$, x+y=3, Ru 1.5%$_{w/w}$; Rh/C, Pt/C, and Ru/C were obtained from Sigma Aldrich (5%$_{w/w}$; cod. 206164, 330159, and 84031, respectively). Dodecane was obtained from Fluka.

Methods

Catalyst preparation

The Pt/Ru/K1221 catalyst was prepared by the impregnation procedure described in the main article, whereby the amounts stated in Table S1 were employed.

Table S2 Quantities used in the preparation of polymer-supported catalysts (Step 1/2)

Metal	Step	Reagent	Quantity [g]	Quantity [mmol]	Water [ml]
Pt	1	$[Pt(NH_3)_4](NO_3)_2$	0.492	1.27	30
Ru		$[Ru(NO)(NO_3)_x(OH)_y]$ [1]	8.561	1.27	0
	2	$NaBH_4$	1.005	26.6	5

[1] x+y=3, aqueous solution, 1.5%$_{w/w}$ of Ru; [2] aqueous solution, 10%$_{w/w}$ of Ru; 5%$_{w/w}$ HNO_3, 2.727 g solution used

Catalyst characterisation

To determine the ion exchange capacity, the beads (2.17 g) were suspended in deionized water (100 ml) for 2 h. Aqueous NaOH (1M) was added until the pH-value was basic; subsequently, the mixture was stirred for 30 min, filtered, and the excess NaOH was back-titrated with aqueous HCl (1M).

The size of the polymer beads was determined optically on a *Keyence VHX DIGITAL MICROSCOPE* or *VHX-1000* microscope (magnification from 50× to 500×). Furthermore, a 3D image was obtained on a *STEMI2000C Zeiss stereo-microscope*.

The metal content of M/K1221 was determined after microwave assisted (CEM MARS Xpress) dissolution of the sample (50 mg) in aqueous HNO_3 (10 cm^3) by inductively coupled plasma atomic emission spectrometry (ICP-OES) using a Spectro Ciros Vision, ICP-OES instrument.

Scanning electron microscopy (SEM) and energy dispersive X-ray analysis (EDAX) were carried out using a Hitachi UHR FE-SEM SU9000 and Oxford Instrument, respectively. Powder X-ray diffraction studies were carried out using an Empyrean instrument from PANalytical X-ray diffractometer.

The WAXS analysis were done by using a Cu X-ray tube (line source of 12×0.04 mm^2) which provided CuKα radiation with λ=0.1542 nm. The K_β line was removed by a Ni filter. Source and detector moved in the vertical direction around a fixed horizontal sample. After passing a divergence slit of 1/8° and an anti-scatter slit of 1/4°, the beam reached the sample at the centre of a phi-chi-z stage. In the Bragg-Bretano geometry used, the beam was refocused at a secondary divergence slit of 1/4°. Finally, the signal was recorded by a pixel detector (256×256 pixels of 55 μm) as a function of the scattering angle 2θ. Subsequently, the peak positions were calculated from $q=2\pi/d=(4\pi/\lambda)\sin\theta$, in which q is the scattering vector. The detector was used in a scanning geometry that allowed all rows to be used simultaneously. For each new measurement the height of the (powder) sample was optimized. Scans were made with 2θ, the detector axis, moving at twice the rate of the θ-axis of the incident beam. The calibration was checked using a Si reference sample. The resolution of the total setup was determined by measuring a high-quality Si-wafer, which gave a resolution-limited peak with a full-width-at-half-maximum of 0.026°.

For measuring the solvent accessible molecular volume, a sample of the polymer beads was suspended in a large volume of tetrahydrofuran (THF) for 10 h. Then, excess THF was removed by decantation and a solvent mixture added. For three times, the solvent mixture was exchanged after leaving the suspension standing for three hours. The sample was kept covered by the solvent until just before the measurement.

The porosity of K1221 in water was determined with inverse size exclusion chromatography. The swollen polymer beads were packed as stationary phase. Substances of known molecular size were taken as eluate (Deuterium oxide, Aldrich (cod. 613444) 99.9 atom % D; D-(-)-Ribose, Aldrich (cod. R1757); D-(+)-Xylose, Aldrich (cod. W360600) ≥99%; Sucrose, Sigma (cod. S8501) ≥99.5%; D-(+)-Raffinose, Sigma (cod. R0250) pentahydrated; Dextran, Sigma (cod. 31388) from Laeuconostoc. spp, Mr ~ 6.000; Dextran, Sigma (cod. 95771) from Laeuconostoc. spp, Mr ~ 2.000.000). From the elution volumes

the pore size distribution of the stationary phase was reconstructed.

GC analyses

Samples of the reaction mixture were analysed by gas chromatography using a HP 6890 Series GC System equipped with 50 m CP-Sil-PONA-CB 0.21mm column and FID detector (Method: 50°C for 5 min; 50-250°C, 10°C/min; 250°C 20 min). Dodecane was used as internal standard. The chromatograms were analysed with the software *EZChrome 2.0*. Based on the GC data, different reaction parameters, such as conversion (*X*), product concentrations (*c*), selectivity (*S*), yield (*Y*), ratio between primary and secondary products and between primary and secondary amines were calculated according to the following Eq. 1-5, where MM_i is the molar mass of compound *i*:

$$\boldsymbol{X_{n/n}}\%\,(\boldsymbol{t}) = \frac{\boldsymbol{RF_{NB}\cdot A_{NB}/MM_{NB}}}{\boldsymbol{\sum_i RF_i\cdot A_i/MM_i}} \cdot \mathbf{100} \qquad \textbf{Eq. 1}$$

$$\boldsymbol{c_{j_{n/n}}}\%\,(\boldsymbol{t}) = \frac{\boldsymbol{RF_j\cdot A_i/MM_i}}{\boldsymbol{\sum_i RF_i\cdot A_i/MM_i}} \cdot \mathbf{100} \qquad \textbf{Eq. 2}$$

$$\boldsymbol{S_{j_{n/n}}}\%\,(\boldsymbol{t}) = \frac{\boldsymbol{RF_j\cdot A_j/MM_j}}{\boldsymbol{\sum_{i\neq NB} RF_i\cdot A_i/MM_i}} \cdot \mathbf{100} \qquad \textbf{Eq. 3}$$

$$\boldsymbol{Y_{n/n}}\%\,(\boldsymbol{t}) = \boldsymbol{S_{j_{n/n}}}\%\,(\boldsymbol{t}) \cdot \boldsymbol{X_{n/n}}\%\,(\boldsymbol{t}) \qquad \textbf{Eq. 4}$$

$$\frac{\boldsymbol{CHA}}{\boldsymbol{DCHA}} = \frac{\boldsymbol{c_{CHA}(t)}}{\boldsymbol{c_{DCHA}(t)}} \qquad \textbf{Eq. 5}$$

The respective retention times of the relevant compounds *i* were as follows: CHA (12.2 min), CHO (12.9 min), ANI (15.0 min), NB (17.6 min), DCHA (24.2 min), imine of CHA (24.6 min), BHT (THF inhibitor, 25.5 min), *N*-CHA (26.2 min) and DPA (27.2 min), azoxybenzene (27.2 min), azobenzene (30.0 min). The retention time of dodecane was 20 min.

Kinetic investigation

Kinetic data were calculated from the time-concentration profiles using Runge-Kutta-Method implemented in *Microsoft Excel*. The general way of working was based on a numerical fit of the experimental data using the *Solver* module of *Microsoft Excel*. This is exemplified below for a general reaction A→B. The concentration profile is described by the differential equation 6.

$$\frac{dc_B}{dt} = k^B c_A \qquad \textbf{Eq. 6}$$

Given the assumptions that $dc_B \approx \Delta c_B$ and $dt \approx \Delta t$ and $c_A(t_i) \approx c_A(t_{i-1})$ for sufficiently small increments in concentration and time, the equation can be re-written to equation 7, where Δt is the time interval considered and $c(t_i)$and $c(t_{i-1})$ are the concentrations at time t_i or t_{i-1}, respectively.

$$c_B(t_i) = c_B(t_{i-1}) + k^B c_A(t_{i-1})\Delta t \qquad \textbf{Eq. 7}$$

By repeatedly applying this equation, the concentration of $c_B(t_i)$ was calculated from $c_B(t_{i-1})$. Starting with an initial guess for the parameters k^B, the least squares sum between the experimental and the calculated data was minimized.

The time-concentration profiles of polymer supported catalysts were fitted accordingly using differential equations 8 a-c, 9 a-c and 10 a-c to describe the profile in Phase I, II and III, respectively.

$$\frac{dc_{NB}}{dt} = -k^{I,NB} c_{NB} \qquad \textbf{Eq. 8a}$$

$$\frac{dc_{AN}}{dt} = k^{I,AN} c_{NB} \qquad \textbf{Eq. 8b}$$

$$\frac{dc_{CHA}}{dt} = k^{I,CHA} c_{NB} \qquad \textbf{Eq. 8c}$$

$$\frac{dc_{NB}}{dt} = -k^{II,NB} \qquad \textbf{Eq. 9a}$$

$$\frac{dc_{AN}}{dt} = k^{II,AN} \qquad \textbf{Eq. 9b}$$

$$\frac{dc_{CHA}}{dt} = k^{II,CHA} \qquad \textbf{Eq. 9c}$$

$$\frac{dc_{NB}}{dt} = -k^{III,NB} c_{NB}^2 \qquad \textbf{Eq. 10a}$$

$$\frac{dc_{AN}}{dt} = k^{III,AN} c_{NB}^2 \qquad \textbf{Eq. 10b}$$

$$\frac{dc_{CHA}}{dt} = k^{III,CHA} c_{NB}^2 \qquad \textbf{Eq. 10c}$$

The parameter variation was started from different initial values for the kinetic constants to avoid local minima.

Supplementary Information

Catalyst characterisation

Optical micrographs of the parent K1221 and Rh/K1221 beads are shown in Figure S1.

Figure S1. Chemical structure of the K1221 ionic exchange resin (left); images of the parent K1221 beads (top right) and of the Rh/K1221 beads after immobilization of the metal nanoparticles (bottom right).

The morphology of the Rh, Pt, Ru, and Ni nanoparticles formed inside the K1221 network was studied by X-ray diffraction (Figure S2) and scanning electron microscopy (Figure S3).

RSC Advances

Dynamic Article Links ►

Cite this: DOI: 10.1039/c0xx00000x

www.rsc.org/xxxxxx

ARTICLE TYPE

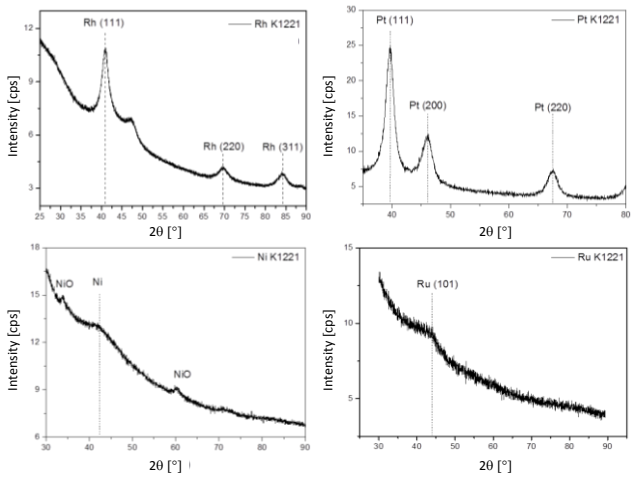

Figure S2. Powder X-ray diffraction analysis of Rh/K1221, Pt/K1221, Ru/K1221 Ni/K1221 (clockwise, Rh top left)

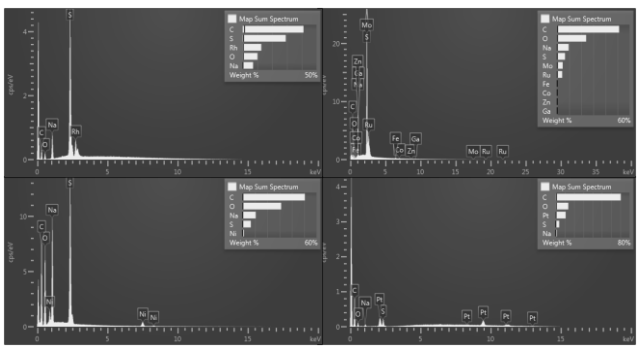

Figure S3. EDX analysis of Rh/K1221, Pt/K1221, Ru/K1221 Ni/K1221 (clockwise, Rh top left)

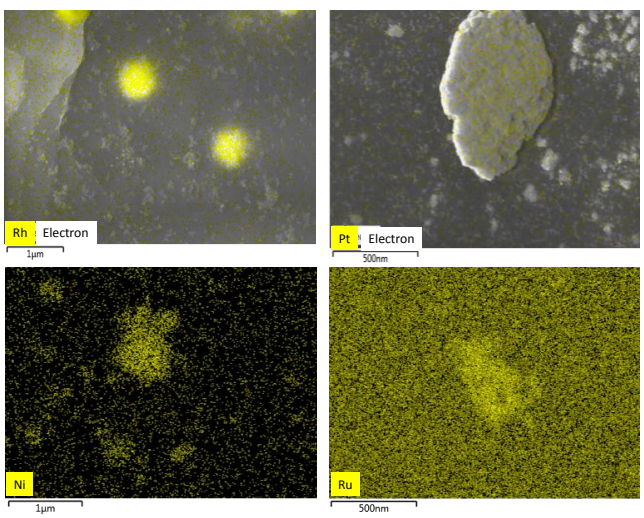

Figure S4. EDS images of the inside of a cut bead of Rh/K1221, Pt/K1221, Ru/K1221 Ni/K1221 (clockwise, Rh top left)

To check the reproducibility of the measurement of the solvent accessible molecular volume, the uptake of reactants, products and solvents into polymer beads was determined for three times (Figure S4).

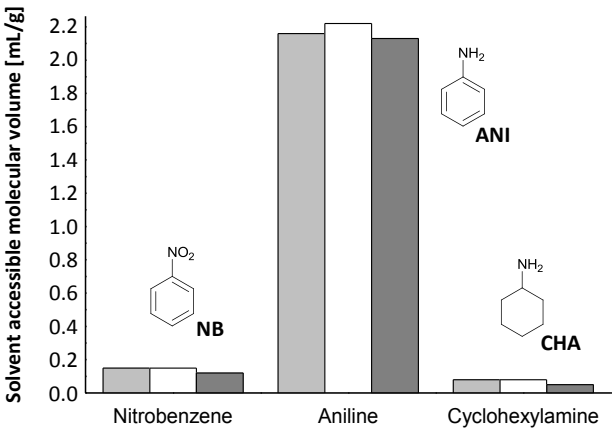

Figure S5. Reproducibility of the measurement on the solvent accessible molecular volume (SAV) for the uptake of nitrobenzene, aniline and cyclohexylamine into the Pt/Ru/K1221 beads.

Kinetic investigation

The formation of primary and secondary products was analysed for Rh/K1221 by plotting the ratios of the concentrations of cyclohexylamine/aniline, dicyclohexylamine/cyclohexylamine, N-cyclohexylaniline/cyclohexylamine and of diphenylamine/aniline *vs.* time (Figure S5).[62] During phase I, the ratio cyclohexylamine/aniline extrapolated to zero time converged against zero. From this, it was inferred that during this phase cyclohexylamine is a consecutive product of aniline. In all other cases, the ratio extrapolated to zero time converged against a specific value not equal to zero or infinity. From this, it was inferred that aniline and cyclohexylamine (phase II and III), cyclohexylamine and dicyclohexylamine (all phases), *N*-cyclohexylaniline and cyclohexylamine (phase II and III) and diphenylamine and aniline (phase II and III) were formed as parallel products.

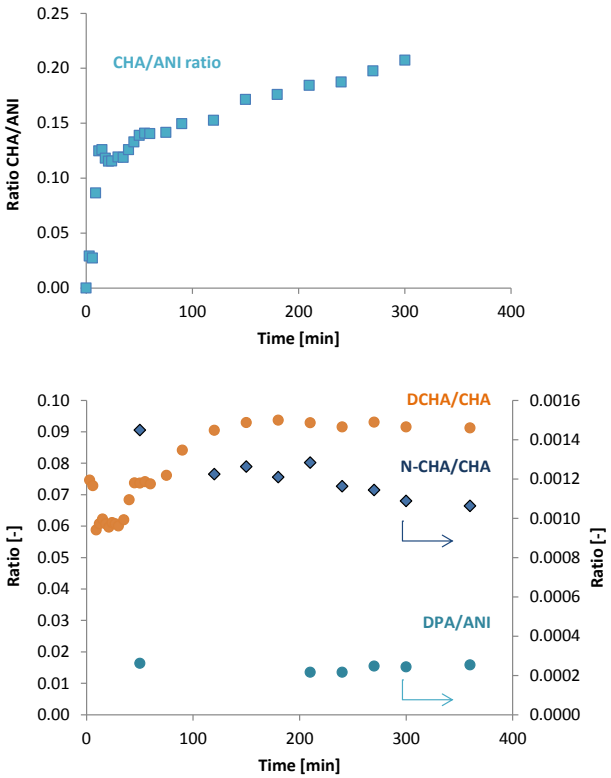

Figure S6. Ratio of each two of the products formed during the hydrogenation of nitrobenzene over Rh/K1221 (120°C, 100 bar, s/m 500, THF/MeOH/ 9:1); CHA: cyclohexylamine, ANI: aniline, DCHA: dicyclohexylamine, N-CHA: *N*-cyclohexylaniline, DPA: diphenylamine

The time-concentration profile for and Pt/K1221, Ru/K1221, and Ni/K1221 is given in Figure S7 and for Pt/C, Ru/C, and Ni/C in Figure S8.

The initial rates, conversions and selectivities towards the products obtained with catalyst mixtures and polymer-supported alloys of Ru/Pt and Ni/Rh are given in Table S2.

Table S2 Initial rate, conversion and selectivity of nitrobenzene hydrogenation over mixtures of polymer-supported metal nanoparticles and polymer-supported alloys of Ru/Pt and Rh/Ni on K1221

Catalyst	Initial rate [a] [10^3 $mol_{NB} \cdot mol_M^{-1} \cdot h^{-1}$]				Conv.[b] [%]	Selectivity[b] [%]		
	NB	ANI	CHA	DCHA		ANI	CHA	DCHA
Ru/K1221 Ni/K1221	-1.1	1.0	0.1	0.01	77	77	22	1.1
Rh/K1221 Ru/K1221	-1.2	1.0	0.1	0.01	70	77	21	1.9
Pt/K1221 Ru/K1221	-1.3	1.2	0.1	0.01	70	80	19	1.0
Pt/K1221 Ni/K1221	-1.7	1.4	0.2	0.01	78	80	19	0.9
Pt/K1221 Rh/K1221	-1.4	1.2	0.2	0.01	79	75	24	1.2
Rh/K1221 Ni/K1221	-1.2	1.0	0.1	0.01	67	79	19	1.5
Pt/Ru/K1221	-1.2	1.0	0.2	0.01	69	77	21	1.9
Rh/Ni/K1221	-1.2	1.0	0.2	0.01	64	74	24	2.0

[a] 120°C, 100 bar, s/m 500, THF/MeOH 9:1; [b] after 360 min; NB: nitrobenzene; ANI: aniline; CHA: cyclohexylamine; DCHA: dicyclohexylamine

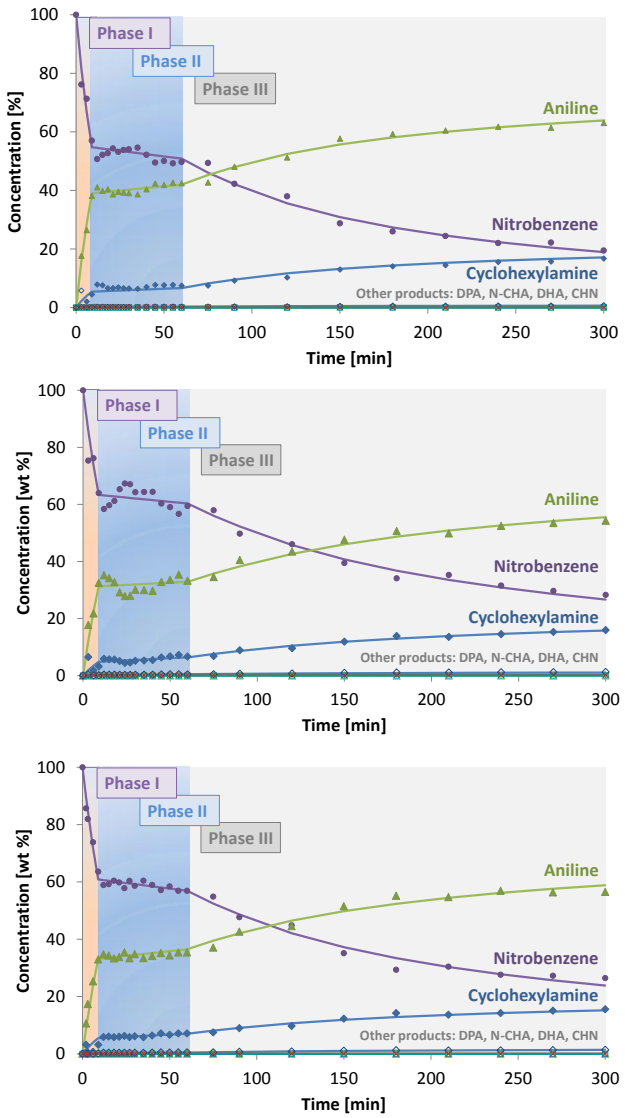

Figure S7. Time-concentration profile of the hydrogenation of nitrobenzene over Pt/K1221 (top), Ru/K1221 (middle) and Ni/K1221 (bottom) (120°C, 100 bar, s/m 500, THF/MeOH 9:1)

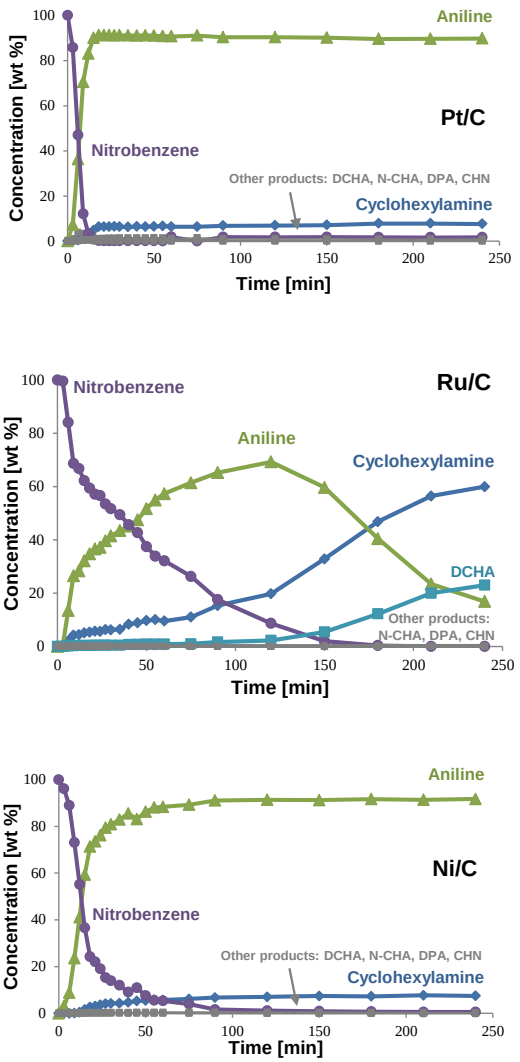

Figure S8. Time-concentration profile of the hydrogenation of nitrobenzene over the carbon-supported catalysts Pt/C (top), Ru/C (middle) and Ni/C (bottom) (120°C, 100 bar, s/m 500, THF/MeOH 9:1)

RSC Advances

Dynamic Article Links ►

Cite this: DOI: 10.1039/c0xx00000x

www.rsc.org/xxxxxx

ARTICLE TYPE